INSTITUTE OF PHYSICS PUBLISHING JOURNAL OF PHYSICS B: ATOMIC, MOLECULAR AND OPTICAL PHYSICS

J. Phys. B: At. Mol. Opt. Phys. **39** (2006) 2949–2957 doi:10.1088/0953-4075/39/14/003

A stable ac current source for magnetic traps

K L Baranowski and C A Sackett

Department of Physics, University of Virginia, Charlottesville, VA, 22904, USA

E-mail: sackett@virginia.edu

Received 31 March 2006, in final form 23 May 2006
Published 30 June 2006
Online at stacks.iop.org/JPhysB/39/2949

Abstract

A power source is presented capable of providing ac currents with amplitudes of up to 50 A and frequencies near 10 kHz. The current amplification is actively stabilized and exhibits fractional current noise better than one part in 10^5. The source was developed for use with an atom interferometer based on magnetically trapped condensate atoms. The relationship between current noise and interferometer noise is developed, and it is shown that the demonstrated precision should permit interferometry with coherence times of 1 s or more.

1. Introduction

A considerable effort is currently underway to develop atom interferometers using magnetically trapped Bose–Einstein condensates [1–5]. Such devices have the potential to be compact and portable sensors, useful for applications in inertial navigation and gravitational measurements [6, 7]. However, many technical problems remain to be solved before this promise can be realized. One straightforward issue is the effects of magnetic field noise. Fluctuating ambient fields can easily induce large phase shifts to the atoms, degrading the interferometer performance. We have argued elsewhere [8] that this effect might be avoided using a time-orbiting potential (TOP) technique. In this case, the atomic spins rotate rapidly in space, so that phase shifts from slowly varying external fields are alternately positive and negative, thus tending to average out.

Of course, this technique introduces susceptibility to noise at the TOP rotation frequency. In particular, fluctuations in the trap field itself will still introduce phase noise. It is therefore important to understand the stability requirements of the trap field and how these may be achieved. Since the trap field is typically generated electromagnetically, one important noise source is the driving current. In this paper, we present a highly stable ac current source which we believe will be well suited for atom interferometry and similar precision experiments. In section 2, we present a general calculation of the relationship between current noise in the trap and phase noise of the interferometer. In section 3, we present our design for a stabilized current source suitable for this purpose. In section 4, we discuss the noise properties of our source, and in section 5 we estimate the achievable phase stability.

 © 2006 IOP Publishing Ltd Printed in the UK

2. Stability requirements

We consider a Michelson interferometer similar to that of [2, 5]. A condensate starts out in a magnetic guide, where it is confined in two dimensions and supported against gravity. The third dimension is free or only weakly confined. Through Bragg scattering [9, 10], an off-resonant standing wave laser beam splits the condensate into two packets travelling in opposite directions down the guide. After the packets propagate for time $T/4$ the Bragg beam is again applied so as to reverse their motion. The packets travel back for time $T/2$ and are then reflected once again. After time $T/4$ they have returned to their initial location and the Bragg beam is applied a final time, reversing the initial splitting operation. The fraction of atoms brought back to rest depends on the difference in quantum phase between the two packets. Our goal is to determine how stable the magnetic field of the guide must be in order to minimize its contribution to the measurement.

The phase acquired by a single packet is

$$\phi_1 = \frac{1}{\hbar}\int_{-T/2}^{T/2} E(z_1, t)\,\mathrm{d}t \tag{1}$$

where $E(z_1, t)$ is the energy of the packet at position z_1 and at time t. The other packet's motion is described by $z_2(t)$. The final phase difference between the two packets is thus

$$\phi = \phi_1 - \phi_2 = \frac{1}{\hbar}\int_{-T/2}^{T/2} [E(z_1, t) - E(z_2, t)]\,\mathrm{d}t. \tag{2}$$

We suppose here that the energy depends only on the magnetic field of the guide B, so that $E(z, t) = \mu B(z, t)$ for atomic moment μ. Since we are primarily interested in the current stability requirements, we assume further that temporal variations in the field are caused by variations in the current I, so that $B(z, t) = \beta(z)I(t)$. Finally, we decompose the current $I(t) = \bar{I}[1 + \eta(t)]$, where $\bar{I}$ is deterministic and here assumed constant. The noise term $\eta(t)$ satisfies $\langle\eta\rangle = 0$. Since the packets complete a full oscillation in the potential, any phase due to $\bar{I}$ will be the same for both packets and thus cancel. Then

$$\phi = \frac{\mu\bar{I}}{\hbar}\int_{-T/2}^{T/2} [\beta(z_1) - \beta(z_2)]\eta(t)\,\mathrm{d}t. \tag{3}$$

The phase variance is given by $\Delta\phi^2 = \langle\phi^2\rangle - \langle\phi\rangle^2 = \langle\phi^2\rangle$, or

$$\Delta\phi^2 = \frac{\mu^2\bar{I}^2}{\hbar^2}\iint [\beta(z_1) - \beta(z_2)][\beta(z_1') - \beta(z_2')]\langle\eta(t)\eta(t')\rangle\,\mathrm{d}t\,\mathrm{d}t' \tag{4}$$

where z_1' indicates $z_1(t')$, etc.

We express β using a Taylor expansion,

$$\beta(z) = \sum_{n=0}^{\infty} \beta_n z^n, \tag{5}$$

and we suppose that the field variation is weak enough that the atomic motion is not significantly affected by it. Then since $z_1(t) = -z_2(t)$, terms with even powers of z will generate no net phase shift. The lowest contributing term is the linear gradient, $n = 1$. However, if the guide also provides weak harmonic confinement ($\beta_2 > 0$), then the initial condensate location will normally be at the minimum of the potential and β_1 will be zero. We assume that either the $n = 1$ or $n = 3$ term will dominate, and keep only this leading term $\beta_n z^n$, so that

$$\beta(z_1) - \beta(z_2) \approx 2\beta_n z_1^n. \tag{6}$$

Substituting (6) into equation (4) yields

$$\Delta\phi^2 \approx \frac{4\mu^2\bar{I}^2}{\hbar^2}\beta_n^2 \iint z_1^n z_1'^m \langle \eta(t)\eta(t')\rangle \,\mathrm{d}t\,\mathrm{d}t'. \tag{7}$$

For a stationary noise distribution, the autocorrelation function $\langle \eta(t)\eta(t')\rangle$ can be written as $\Gamma(\tau)$ with $\tau = t - t'$. It is related to the noise spectrum via the Weiner–Khintchine theorem

$$\Gamma(\tau) = \int_{-\infty}^{\infty} S^{(2)}(\nu)\,\mathrm{e}^{-2\pi\mathrm{i}\nu\tau}\,\mathrm{d}\nu. \tag{8}$$

Here $S^{(2)}(\nu)$ is the double-sided power spectral density of the noise as a function of the frequency ν. However, for comparison with experimental data, it is more convenient to use the single-sided power spectrum,

$$S(\nu)\begin{cases} 0 & \text{for } \nu < 0 \\ 2S^{(2)}(\nu) & \text{for } \nu \geqslant 0. \end{cases} \tag{9}$$

Since η is the fractional noise, S has dimensions 1/Hz, and it can be determined from a measured current noise spectrum S_I by $S = S_I/\bar{I}^2$. It permits equation (7) to be expressed as

$$\Delta\phi^2 = \frac{4\mu^2\bar{I}^2}{\hbar^2}\beta_n^2 \int_0^{\infty} S(\nu)\tilde{h}_n(\nu)\,\mathrm{d}\nu \tag{10}$$

where

$$\tilde{h}_n(\nu) = \left|\int_{-T/2}^{T/2} z_1(t)^n\,\mathrm{e}^{-2\pi\mathrm{i}\nu t}\,\mathrm{d}t\right|^2. \tag{11}$$

It is convenient to normalize $\tilde{h}_n$ as $\tilde{h}_n(\nu) = H_n h_n(\nu)$ with $\int h_n\,\mathrm{d}\nu = 1$. The normalization factor H_n can be expressed simply as

$$H_n = \int_{-T/2}^{T/2} z_1(t)^{2n}\,\mathrm{d}t, \tag{12}$$

which can be obtained by integrating (11) with respect to ν.

For the experiment considered here, the packet position z_1 is given by

$$z_1(t)\begin{cases} v\left(t + \frac{T}{2}\right) & \text{if } \frac{-T}{2} < t < \frac{-T}{4}, \\ -vt & \text{if } \frac{-T}{4} < t < \frac{T}{4}, \\ v\left(t - \frac{T}{2}\right) & \text{if } \frac{T}{4} < t < \frac{T}{2} \end{cases} \tag{13}$$

where $v = 2\hbar k/M$ is the Bragg velocity for light with wavenumber k and atoms with mass M. In this case,

$$H_n = \frac{v^{2n}T^{2n+1}}{(2n+1)2^{4n}} \tag{14}$$

and for $u \equiv \pi\nu T/2$,

$$h_1 = \frac{3T}{4u^4}(\sin 2u - 2\sin u)^2 \tag{15}$$

$$h_3 = \frac{63T}{u^8}(\sin 2u - 2\sin u + u^2\sin u)^2. \tag{16}$$

These functions are plotted in figure 1. They permit the interferometer measurement noise to be estimated if the current noise density S and the relevant guide field moment β_n are known.

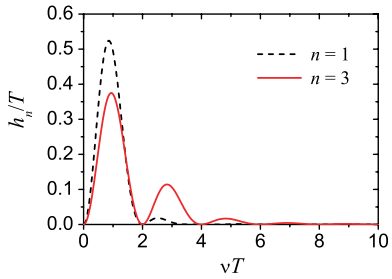

Figure 1. Noise sensitivity functions for the atom interferometer, as functions of νT for frequency ν and measurement time T. The dashed curve corresponds to a waveguide with a linear potential gradient and the solid curve to a guide with cubic variation.

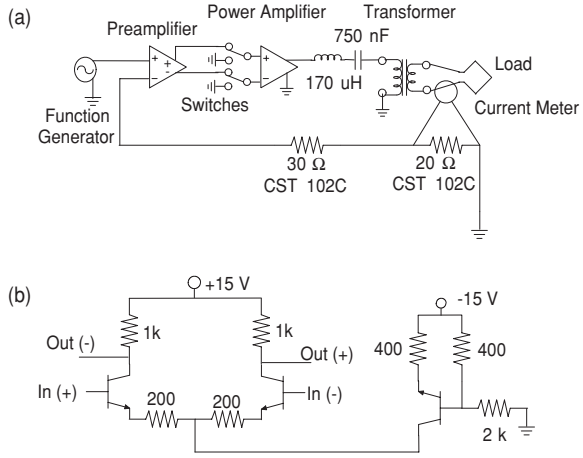

Figure 2. (a) Stabilized current source circuit schematic. (b) Preamplifier circuit.

3. Current source implementation

The magnetic guide used in our experiment is described in [8]. Since it is based on a time-orbiting potential (TOP) technique, it requires ac current. In fact, it uses three separate circuits: two to generate a rotating bias field and one for an oscillating linear quadrupole. We operate at a TOP frequency of 11.9 kHz. The three trap circuits have similar complex impedances at this frequency, with magnitudes of 25 mΩ and phases of 66°. The circuits require currents with amplitudes of up to 50 A.

To power these circuits, we designed a stabilized ac current source as shown in figure 2(a). Each circuit is driven with an independent source. A sine wave from an oscillator is first applied to one input of a homebuilt differential pre-amplifier. The signal passes through a switch and is fed into a power amplifier. The output of the amplifier passes through an LC resonator that improves impedance matching to the load and provides increased stability in the servo loop as discussed below. The current is stepped up using a transformer and applied to the trap. The load current is measured using a current sensing transformer, and the sense current is converted to a voltage via precision resistors. Finally, this signal is fed back to the input of the preamp, closing the servo loop.

In more detail, the oscillator is an Agilent 33120 A arbitrary waveform generator, with a phase locking option allowing the phase relationship between the different circuits to be maintained. Its noise properties are discussed below. The preamp circuit is a standard differential amplifier design [11], shown in figure 2(b). It provides a gain of 11 db, and is required because the power amplifier does not have enough gain for the optimum current stabilization. It uses transistors rather than op amps to maintain high speed. The power amplifier is a QSC Audio model RMX 1450 commercial audio amplifier. It has a maximum gain of 32 db and can provide 200 W of power to a 4 Ω load. The gain can be conveniently attenuated using the volume knob.

The LC resonator is tuned to make the entire load resonant at 11.9 kHz. The resonator consists of a 750 nF polypropylene power capacitor and 170 μH toroidal inductor home made from litz wire. The inductor has a resistance of about 0.5 Ω, and the impedance of the total load on resonance is 1.8 Ω.

The power transformer (West Coast Magnetics model WCM406 E28) has a 10:1 winding ratio and a power transfer efficiency of about 75%.

The current sense transformer (Triad Magnetics CST206-3A) has a 200:1 turn ratio. By comparing the sense currents from two transformers measuring the same primary current, we found the sense transformer output to drift by less than one part per million over a several minute time scale. The sense transformer drives a Vishay series S102C precision 20 Ω resistor. The sense circuit thus has an output signal of 0.1 V A^{-1}. The resistor has a specified temperature coefficient of 2 ppm $^{\circ}C^{-1}$, which is necessary because variations in this resistance cause the output current to drift. The additional 30 Ω resistor in series makes the sense circuit source impedance 50 Ω, matching that of the oscillator source and improving the balance of the preamplifier.

The stability of the system requires careful attention [12], since the operating frequency is near the 20 kHz nominal maximum frequency of the power amplifier. The feedback loop gain is

$$H = G_0 G_1 \frac{Z_F}{Z_L} \tag{17}$$

where G_0 is the preamplifier gain, G_1 the power amplifier gain, Z_F is the effective feedback impedance, and Z_L is the load impedance. Accounting for the transformer, the feedback impedance Z_F is 10×0.1 V $A^{-1} = 1$ Ω. At high frequencies, the total load acts essentially as an $L = 200$ μH inductor, with an impedance $Z_L = i2\pi\nu L$ for frequency ν. The preamplifier has a constant gain across the frequencies of relevance, with a slowly growing phase shift that reaches -8° at 100 kHz. The power amplifier gain is reduced by 3 db at a frequency of 80 kHz, at which point its phase shift has reached -80°.

For the circuit to be stable, the loop gain must fall below 0 db before the total phase shift reaches -180°, which occurs at about 80 kHz. The maximum loop gain at that frequency is +3 db (+43 db for the amplifiers and −40 db for the inductor). This agrees well with the observed fact that the power amplifier gain must be attenuated by at least 4 db in order to have stable operation. We typically use an attenuation of 8 db to provide a margin of safety and improve the circuit's transient response.

With 8 db attenuation, the loop gain at 11.9 kHz is about 30 db. It is desirable for this gain to be high so that the sense signal follows the input signal as closely as possible. The servo error is $1/(1 + H)$, or 0.03 in our case. We can therefore expect to reduce by a factor of 30 any current fluctuations caused by drifts in the amplifier gains or load impedance. The error could be reduced further by using faster amplifiers or by increasing the amplifier gain and the resonator inductance (while adjusting the capacitor to keep the resonance frequency correct). Increasing the inductance, however, would also make the circuit respond more slowly when

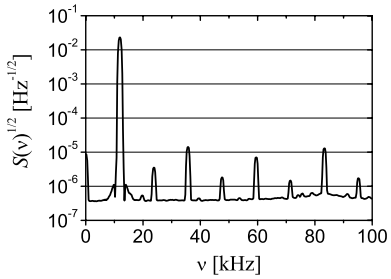

Figure 3. An output spectrum of current source. A single current source was set to 25 A amplitude and monitored with a current sense transformer. The sense voltage was observed with a spectrum analyser and the power spectrum recorded. The plotted values are normalized by the amplitude of the monitor signal, and the measurement linewidth was 250 Hz.

switched on and off. The circuit described here has a measured turn-on time of 60 μs and turn-off time of 150 μs.

4. Noise measurements

Since the magnetic field of our guide rotates, the field magnitude in the trap depends on the amplitude of the oscillating current, rather than the current itself. This slightly changes the interpretation of the results of section 1. The two components of the field are driven by currents $I_1 = (\bar{I} + \delta_1)\cos(\omega t + \alpha_1)$ and $I_2 = (\bar{I} + \delta_2)\sin(\omega t + \alpha_2)$, where the δ's and α's are the noise terms. The magnetic field magnitude is proportional to $I \equiv \left(I_1^2 + I_2^2\right)^{1/2}$. To first order, this is

$$I \approx \bar{I} + \delta_1 \cos^2 \omega t + \delta_2 \sin^2 \omega t + (\alpha_2 - \alpha_1)\cos \omega t \sin \omega t. \tag{18}$$

As indicated in figure 1, the interferometer phase is insensitive to noise that is very fast compared to T^{-1}. Considering typical values for T of 10 ms or greater, the oscillating terms in (18) will have little effect. Averaging over them yields

$$I \approx \bar{I} + \frac{\delta_1 + \delta_2}{2} \approx \bar{I} + \delta_1 \tag{19}$$

assuming that the two currents have similar noise properties. This has the same form as used in section 1, but with $\eta = \delta_1/\bar{I}$ corresponding to the amplitude noise of the current.

We characterized the current noise in several ways. Figure 3 shows the spectrum of the current over a wide frequency range. We monitored the current using a sense transformer of the same type used in the driver circuit. From this data, the total harmonic distortion of the source is determined to be 0.2%, which is consistent with the specifications of the power amplifier. Harmonic distortions cause high frequency modulation of the field similar to that in equation (18), but this is again not expected to be important for the interferometer. The figure also shows some enhancement of noise near 80 kHz, which is due to the low phase margin of the servo loop there.

To accurately measure the current noise near the oscillation frequency, we used the method shown in figure 4. To reduce the dynamic range of the signal, we monitored two circuits together. The currents from both circuits passed through a single sense transformer, and the phases of the two circuits were set 180° apart so that the main signal amplitudes mostly cancelled. The sources are assumed to have uncorrelated noise, making the measured noise $2^{1/2}$ times larger than that of a single source. The reported results are corrected for this factor.

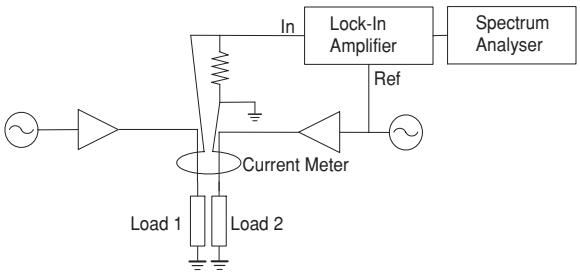

Figure 4. Setup for measurement of amplitude noise. The currents from two sources with equal amplitudes and the opposite phase were measured simultaneously with a current sense transformer. The sense signal was processed by a lock-in amplifier, using one of the sources as a reference. The output signal from the lock-in was observed on a spectrum analyser.

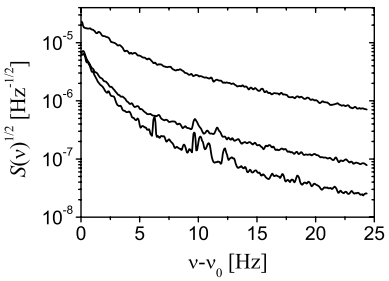

Figure 5. Amplitude noise of the ac current, near $\nu_0 = 11.9$ kHz. Using the circuit of figure 4, the current noise was measured for various configurations. The middle curve shows the results for the complete current source. The upper curve was obtained by disabling the stabilization feedback loop in the source. The lower curve shows the voltage noise of the unamplified oscillators. In each case, the monitor signal amplitude for a single source was set to 1 V.

The monitor signal was measured by a lock-in amplifier, using the signal from one of the oscillators as a reference. With the correct choice of reference phase, this extracted the amplitude noise of the signal but not the phase noise. The lock-in shifted the noise to low frequency, and it was filtered with a time constant of 10 ms. This filtered output was then passed to a spectrum analyser, with the results shown as the middle trace in figure 5. This then provides the noise spectrum for use in equation (10).

For comparison, the top trace shows the noise spectrum obtained when the feedback loop of the current source is removed. The stabilization reduces the amplifier noise by about an order of magnitude over most of the range. This is somewhat lower than the factor of 30 predicted by the stability analysis, suggesting that some noise is introduced by the feedback elements. The lower trace shows the noise measured for the 33 120 A oscillators by themselves, and indicates that source noise is the dominant factor for bandwidths below a few Hz.

As a final method to characterize the noise, we monitored the drift of the current amplitude over time. We again monitored two opposing sources as in figure 4, but in this case we rectified the monitor signal and sampled it once per minute using an analogue-to-digital converter. Figure 6 shows the results. The lower trace was measured using the stabilized source, while the upper trace was measured with the feedback loop disabled. The feedback reduces the drift by about a factor of 10, consistent with the improvement seen in figure 5.

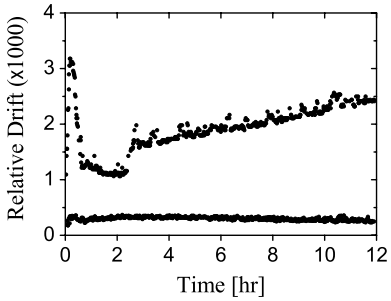

Figure 6. Fractional current drift. Using a double-source setup similar to that of figure 4, the current drift of the sources were monitored. The measured voltages were normalized by the amplitude of the signal from a single source. The lower trace shows the results of the stabilized system while the upper trace shows the results when the feedback loop is disabled. In both cases, the current was turned on at time zero, after having been off over night. The current amplitude was 23 A.

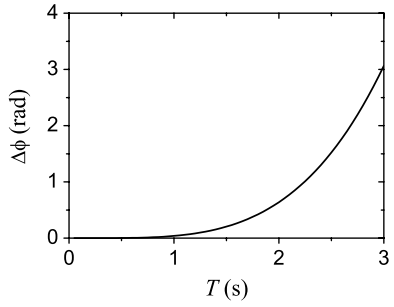

Figure 7. Interferometer noise due to current fluctuations, as a function of measurement time T. The phase noise $\Delta\phi$ from equation (10) is evaluated using the noise data of figure 5, for a trap with cubic field dependence and $\beta_3 \bar{I} = 5\ \mathrm{T\ m^{-3}}$.

5. Interferometer performance and conclusions

The spectrum of figure 5 provides the noise data necessary to evaluate the interferometer phase noise (10). The remaining unknown quantity is the field coefficient β_n. In our experiment, the atoms are weakly confined along the guide axis by a harmonic potential, so there is no linear term and we consider the cubic term β_3. We do not observe any anharmonicity in the atomic motion in our trap, so we have no direct measurement of the cubic term. However, in designing the trap we developed a numerical model for the fields, as described in [8]. This model predicts the measured bias field and quadratic field coefficient with an accuracy of about 10%. It indicates a β_3 coefficient of 0.1 $(\mathrm{T\ m^{-3}})\ \mathrm{A^{-1}}$.

Figure 7 shows the resulting phase noise $\Delta\phi$, for a current amplitude of 50 A and for atoms in a state with $\mu = \mu_\mathrm{B}$, the Bohr magneton. As seen, noise from the current fluctuations should be negligible up to interaction times of about 1 s, after which the effect rapidly grows.

An interaction time of 1 s is long enough for a variety of precision measurements. By measuring 10^5 Rb atoms with shot-noise limited precision, an interferometer configured for gravitational measurements could determine g to a precision of 4×10^{-11}, or a Sagnac interferometer could determine rotation rates with a precision of 3×10^{-8} rad $\mathrm{s^{-1}}$. Achieving

such results with atoms confined in a magnetic guide will require careful elimination of many noise sources, but the results reported here show that noise due to current fluctuations does not present an insurmountable obstacle.

Acknowledgments

We would like to thank R R Jones for fruitful discussions. This work was supported by the US Office of Naval Research, the National Science Foundation, and the Sloan Foundation.

References

[1] Arnold A S 2004 *J. Phys. B: At. Mol. Opt. Phys.* **37** L29
[2] Wang Y J, Anderson D Z, Bright V M, Cornell E A, Diot Q, Kishimoto T, Prentiss M, Saravanan R A, Segal S R and Wu S 2005 *Phys. Rev. Lett.* **94** 090405
[3] Gupta S, Murch K W, Moore K L, Purdy T P and Stamper-Kurn D M 2005 *Phys. Rev. Lett.* **95** 143201
[4] Crookston M B, Baker P M and Robinson M P 2005 *J. Phys. B: At. Mol. Opt. Phys.* **38** 3289
[5] Garcia O, Deissler B, Hughes K J, Reeves J M and Sackett C A 2006 *Preprint* cond-mat/0603772
[6] Gustavson T L, Landragin A and Kasevich M A 2000 *Class. Quantum Grav.* **17** 2385
[7] Peters A, Chung K Y and Chu S 2001 *Metrologia* **38** 25
[8] Reeves J M, Garcia O, Deissler B, Baranowski K L, Hughes K J and Sackett C A 2005 *Phys. Rev.* A **72** 051605
[9] Kozuma M, Deng L, Hagley E W, Wen J, Lutwak R, Helmerson K, Rolson S L and Phillips W D 1999 *Phys. Rev. Lett.* **82** 871
[10] Wu S J, Wang Y J, Diot Q and Prentiss M 2005 *Phys. Rev.* A **71** 043602
[11] Horowitz P and Hill W 1989 *The Art of Electronics* 2nd edn (Cambridge: Cambridge University Press)
[12] Palm W J III 1986 *Control Systems Engineering* (New York: Wiley)